

Excluded-Volume Effects on the Mean-Square Radius of Gyration of Oligo- and Polyisobutylenes in Dilute Solution

Munenori Yamada, Masashi Osa, Takenao Yoshizaki, and Hiromi Yamakawa*

Department of Polymer Chemistry, Kyoto University, Kyoto 606-01, Japan

Received May 27, 1997[®]

ABSTRACT: The mean-square radius of gyration $\langle S^2 \rangle$ was determined from small-angle X-ray scattering and light scattering (LS) measurements for oligo- and polyisobutylenes (PIB) in *n*-heptane at 25.0 °C in the range of the weight-average degree of polymerization x_w from 1.14×10 to 2.48×10^3 . The model parameters of the helical wormlike (HW) chain for PIB are then determined by analyzing simultaneously the present data for $\langle S^2 \rangle/x_w$ and the previous data obtained from LS measurements for samples with large x_w in the same solvent condition and also in isoamyl isovalerate at 25.0 °C (Θ), by the use of the HW theories with and without the excluded-volume effect. With the parameter values so determined for PIB, the plots of the viscosity- and hydrodynamic-radius expansion factors α_η and α_H against the scaled excluded-volume parameter \tilde{z} for PIB along with those for atactic polystyrene and atactic and isotactic poly(methyl methacrylate)s are shown to form a single-composite curve better than before in each case, confirming the validity of the quasi-two-parameter scheme. The improvement of the consistency of the results for PIB with those for the other polymers arises from the re-evaluation of \tilde{z} with the present values of the model parameters directly determined from $\langle S^2 \rangle$.

Introduction

In a recent experimental paper of this series on the excluded-volume effects in dilute solutions of oligomers and polymers,¹ we have reported the results for the hydrodynamic-radius expansion factor α_H for the hydrodynamic radius R_H defined from the translational diffusion coefficient D for polyisobutylene (PIB).² In conjunction with those for α_H for atactic polystyrene (a-PS)^{3,4} and a- and isotactic (i-) poly(methyl methacrylate)s (PMMA),⁵ it has been confirmed that the quasi-two-parameter (QTP) scheme⁶ is valid for α_H as well as for the gyration-radius^{1,7,8} and viscosity-radius^{7–10} expansion factors α_S and α_η ; i.e., they are functions only of the scaled excluded-volume parameter⁶ \tilde{z} . Strictly, however, the data points for α_H and also α_η plotted against \tilde{z} for PIB deviate somewhat upward from those for a-PS and a- and i-PMMA. As mentioned in the previous paper,² this may probably be due to the fact that the model parameters of the helical wormlike (HW) chain model⁶ for PIB, whose values are required for the evaluation of \tilde{z} , have not been determined directly or correctly from the unperturbed mean-square radius of gyration $\langle S^2 \rangle_\Theta$ at the Θ temperature. The object of the present paper is to determine them directly and reanalyze α_η and α_H for PIB.

In previous experimental studies of $\langle S^2 \rangle_\Theta$,⁹ the intrinsic viscosity $[\eta]_\Theta$,¹¹ and D_Θ ² for PIB at the Θ temperature, isoamyl isovalerate (IAIV) at 25.0 °C and benzene at 25.0 °C were used as the Θ solvents. Unfortunately, however, $\langle S^2 \rangle_\Theta$ for PIB oligomers can be determined from small-angle X-ray scattering (SAXS) measurements neither in IAIV nor in benzene because of the extremely low excess electron density of PIB in them.¹¹ Note also that light scattering (LS) measurements are difficult to carry out for PIB in benzene because of the extremely low refractive index increment. In this paper, therefore, we adopt a *direct* procedure for determining the HW model parameters from $\langle S^2 \rangle$ in Θ and good solvents. It consists of analyzing simultaneously the

previous results for $\langle S^2 \rangle_\Theta$ in IAIV for PIB⁹ with large weight-average molecule weight M_w and those for $\langle S^2 \rangle$ in *n*-heptane at 25.0 °C (good solvent), in which SAXS measurements are possible and are carried out in this work, on the assumption of the QTP scheme with the use of the HW theory of $\langle S^2 \rangle_0$ for the unperturbed chain without excluded volume. This procedure may be justified if $\langle S^2 \rangle_0$ (in *n*-heptane) is equal to $\langle S^2 \rangle_\Theta$ (in IAIV).⁶ From the fact that the values of $[\eta]$ and R_H of the PIB oligomers in *n*-heptane, for which the excluded-volume effect may be ignored, are in good agreement with their respective values in IAIV,^{2,9} the above condition may be considered to hold, although it cannot be directly confirmed, as mentioned above.

Experimental Section

Materials. Most of the PIB samples used in this work are the same as those used in the previous studies of $\langle S^2 \rangle_\Theta$,⁹ $\langle S^2 \rangle$,⁹ $[\eta]_\Theta$,¹¹ $[\eta]$,⁹ D_Θ ,² and D .² The oligomer samples with $M_w < 5 \times 10^3$ are the fractions separated by preparative gel permeation chromatography (GPC) from the original samples prepared by living cationic polymerization and then subjected to dehydrochlorination to remove the terminal chlorine atom. The samples with $M_w > 5 \times 10^3$ are the fractions separated by fractional precipitation from the commercial samples of Enjay Chemical Co., named Vistanex LM-MS. The sample PIB1a is an additional one. The four samples OIB14, OIB18, OIB22, and OIB26a previously^{2,9,11} used had been contaminated somewhat in the course of measurements carried out repeatedly in the previous studies, so that we refractionated them by preparative GPC. The four samples so prepared are designated as OIB14a, OIB18a, OIB22a, and OIB26b, respectively. The values of M_w of the one additional sample and the four repurified samples were determined from LS measurements, as described in the next subsection.

The values of M_w , the weight-average degree of polymerization x_w calculated from M_w , and the ratio of M_w to the number-average molecular weight M_n determined by analytical GPC are listed in Table 1. As seen from the values of M_w/M_n , all the samples are sufficiently narrow in molecular weight distribution. Note that all the samples used in this work have fixed chemical structures at their chain ends independent of M_w , and there is no disorder in their main chain sequences such as branching and dislocation of the methyl side groups, as previously¹¹ mentioned.

[®] Abstract published in *Advance ACS Abstracts*, October 15, 1997.

Table 1. Values of M_w , x_w , and M_w/M_n for Oligo- and Polyisobutylenes

sample	M_w	x_w	M_w/M_n
OIB11 ^a	6.41×10^2	11.4	1.01
OIB14a	8.54×10^2	15.3	1.02
OIB18a	1.08×10^3	19.3	1.02
OIB22a	1.24×10^3	22.1	1.02
OIB26b	1.44×10^3	25.7	1.01
OIB32 ^b	1.81×10^3	32.2	1.04
PIB1a	5.65×10^3	101	1.10
PIB2a	1.81×10^4	323	1.08
PIB3	2.79×10^4	496	1.07
PIB13a	1.39×10^5	2480	1.07

^a M_w of OIB11 had been determined from GPC.¹¹ ^b M_w 's of OIB32 through PIB13a except PIB1a had been determined from LS in *n*-heptane at 25.0 °C.^{2,11}

The solvent *n*-heptane used for LS and SAXS measurements was purified according to a standard procedure.

Light Scattering. LS measurements were carried out in *n*-heptane at 25.0 °C to determine M_w of the samples OIB14a, OIB18a, OIB22a, OIB26b, and PIB1a, and also $\langle S^2 \rangle$ of the sample PIB13a. The apparatus system, experimental procedure, and method of data analysis are the same as those described in the previous paper.¹¹

The values of the refractive index increment $\partial n/\partial c$ measured with a Shimadzu differential refractometer at 436 nm are 0.1323, 0.1353, 0.1375, 0.1382, and 0.1426 cm³/g for OIB14a, OIB18a, OIB22a, OIB26b, and PIB1a, respectively, in *n*-heptane at 25.0 °C. As for PIB13a, we used the value 0.1435 cm³/g of $\partial n/\partial c$ previously¹¹ determined in *n*-heptane at 25.0 °C.

Small-Angle X-ray Scattering. SAXS measurements were carried out for all the samples except for PIB13a in *n*-heptane at 25.0 °C by the use of an Anton Paar Kratky U-slit camera with an incident X-ray of wavelength 1.54 Å (Cu Kα line). The apparatus system and the methods of data acquisition and analysis are the same as those described in a previous paper.¹²

The measurements were performed for five solutions of different concentrations for each polymer sample and for the solvent at scattering angles ranging from 1×10^{-3} rad to a value at which the excess scattering intensity was negligibly small. Corrections for the stability of the X-ray source and the detector electronics were made by measuring the intensity scattered from Lupolene (a platelet of polyethylene) used as a working standard before and after each measurement for a given sample solution and the solvent. The effect of absorption of X-ray by a given solution or the solvent was also corrected for by measuring the intensity scattered from Lupolene with insertion of the solution or solvent between the X-ray source and Lupolene. The degree of absorption increased linearly with increasing solute concentration.

The excess reduced scattering intensity $\Delta I_R(k)$ as a function of the magnitude k of the scattering vector was determined from the observed (smeared) excess reduced intensity by the modified Glatter desmearing method, which consists of expressing the true scattering function in terms of cubic B-spline functions, as described before,¹² where k is given by

$$k = (4\pi/\lambda_0) \sin(\theta/2) \quad (1)$$

with λ_0 the wavelength of the incident X-ray and θ the scattering angle. Then the data for $\Delta I_R(k)$ were analyzed by using the Berry square-root plot to determine the apparent mean-square radius of gyration $\langle S^2 \rangle_s$.¹² Then the $\langle S^2 \rangle$ of the chain contour was obtained from $\langle S^2 \rangle_s$ as before by the use of the equation

$$\langle S^2 \rangle_s = \langle S^2 \rangle + S_c^2 \quad (2)$$

which was derived for a continuous chain having a uniform circular cross section with S_c being the radius of gyration of the cross section.¹² In this work, we make the above correction by adopting the value 6.6 Å² of S_c^2 calculated from the relation $S_c^2 = v_2 M_L / 2\pi N_A$ with N_A the Avogadro constant, v_2 the partial

Table 2. Results of SAXS and LS Measurements on Oligo- and Polyisobutylenes in *n*-Heptane at 25.0 °C

sample	$\langle S^2 \rangle_s^{1/2}$, Å	$\langle S^2 \rangle^{1/2}$, Å
OIB11	6.7 ₄	6.2 ₃
OIB14a	7.9 ₂	7.4 ₉
OIB18a	9.1 ₂	8.7 ₅
OIB22a	10.3	9.9 ₄
OIB26b	11.3	11.0
OIB32	12.8	12.5
PIB1a	23.9	23.7
PIB2a	45.9	45.9
PIB3	57.8	57.8
PIB13a		138

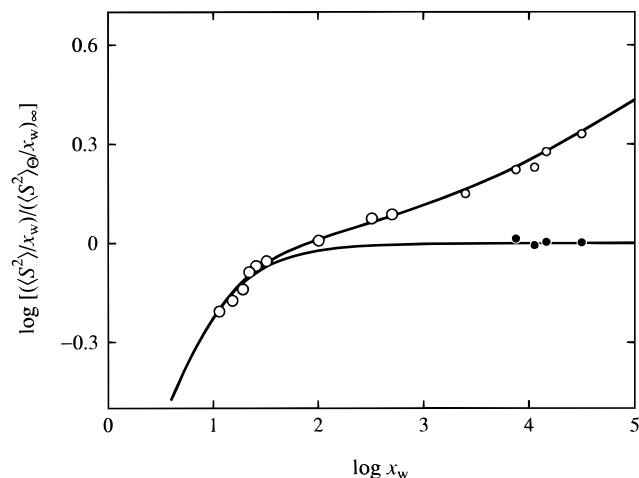


Figure 1. Double-logarithmic plots of $(\langle S^2 \rangle/x_w)/(\langle S^2 \rangle_0/x_w)_\infty$ against x_w for the PIB samples, where $(\langle S^2 \rangle_0/x_w)_\infty$ denotes the asymptotic value of $\langle S^2 \rangle/x_w$ for PIB in IAIV at Θ : (○) present SAXS data in *n*-heptane at 25.0 °C; (○) present and previous LS data in *n*-heptane at 25.0 °C; (●) previous LS data in IAIV at 25.0 °C (Θ). The upper and lower solid curves represent the best-fit YSS and HW theory values for the perturbed and unperturbed chains, respectively (see the text).

specific volume of the polymer, and M_L the shift factor as defined as the molecular weight per unit contour length of the polymer chain. Here, we have used the value 1.04 cm³/g of v_2 previously⁹ determined (although unpublished) for PIB with sufficiently large M_w in *n*-heptane at 25.0 °C and the value 24.1 Å⁻¹ of M_L corresponding to the 8₃ helix.¹¹

The test solutions of each sample were prepared in the same manner as that in the case of LS measurements.¹¹

Results

The values of the apparent root-mean-square radius of gyration $\langle S^2 \rangle_s^{1/2}$ determined from SAXS measurements for the samples OIB11 through PIB3 in *n*-heptane at 25.0 °C are given in the second column of Table 2. In its third column are also given the values of the root-mean-square radius of gyration $\langle S^2 \rangle^{1/2}$ calculated for them from eq 2 with the value of S_c given in the Experimental Section, and also the value determined from LS measurements for the sample PIB13a in the same solvent condition.

Figure 1 shows double-logarithmic plots of $(\langle S^2 \rangle/x_w)/(\langle S^2 \rangle_0/x_w)_\infty$ against x_w for the PIB samples, where $(\langle S^2 \rangle_0/x_w)_\infty$ denotes the asymptotic value of $\langle S^2 \rangle/x_w$ for large x_w . For the convenience of the present procedure of data analysis mentioned in the Introduction, this value for PIB in IAIV at 25.0 °C (Θ) has been evaluated to be 5.48 Å² as an average of the three values of $\langle S^2 \rangle_0/x_w$ previously⁹ determined from LS measurements for the samples PIB60, PIB80, and PIB180 with $x_w = 11\,300$, 14 600, and 31 400, respectively. Those three values along with the one previously⁹ determined similarly for

the sample PIB40 with $x_w = 7540$ are represented by the filled circles in the figure. (The value for PIB40 is less accurate.) We note that the asymptotic value adopted above is only slightly smaller than the value 5.5_3 \AA^2 previously⁹ evaluated as an average of the values for the four samples PIB40 through PIB180, the difference being almost within experimental error. This means that the present values of the model parameters determined in the next section can reproduce the experimental value 5.5_3 \AA^2 of $\langle S^2 \rangle_{\Theta}/x_w$ within experimental error. The large and small unfilled circles represent the present SAXS values and the present and previous⁹ LS ones, respectively, in *n*-heptane at 25.0°C . (The previous LS values for the samples PIB40 through PIB180 are represented by the four small unfilled circles with the highest x_w .) The filled circles represent the previous LS values⁹ in IAIV at 25.0°C (Θ). As mentioned in the Introduction, we may assume that $\langle S^2 \rangle_{\Theta}/x_w$ in IAIV becomes identical with $\langle S^2 \rangle/x_w$ in *n*-heptane for the oligomers with very small x_w . (For the solid curves, see the next section.)

Discussion

Analysis of $\langle S^2 \rangle$ and α_S by the Use of the HW Theory. We begin by briefly summarizing the HW theories⁶ of $\langle S^2 \rangle$ with and without the excluded-volume effect. The HW chain⁶ may be described in terms of four basic model parameters: the differential-geometrical curvature κ_0 and torsion τ_0 of its characteristic helix taken at the minimum zero of its elastic energy, the static stiffness parameter λ^{-1} , and the shift factor M_L .

Now, for the (unperturbed) HW chain of total contour length L without excluded volume, $\langle S^2 \rangle_0$ may be given by^{6,13}

$$\langle S^2 \rangle_0 = \lambda^{-2} f_S(\lambda L; \lambda^{-1} \kappa_0, \lambda^{-1} \tau_0) \quad (3)$$

where the function f_S is defined by

$$f_S(L; \kappa_0, \tau_0) = \frac{\tau_0^2}{\nu^2} f_{S,KP}(L) + \frac{\kappa_0^2}{\nu^2} \left[\frac{L}{3r} \cos \varphi - \frac{1}{r^2} \cos(2\varphi) + \frac{2}{r^3 L} \cos(3\varphi) - \frac{2}{r^4 L^2} \cos(4\varphi) + \frac{2}{r^4 L^2} e^{-2L} \cos(\nu L + 4\varphi) \right] \quad (4)$$

with

$$\nu = (\kappa_0^2 + \tau_0^2)^{1/2} \quad (5)$$

$$r = (4 + \nu^2)^{1/2} \quad (6)$$

$$\varphi = \cos^{-1}(2/r) \quad (7)$$

and with $f_{S,KP}$ being the function f_S for the Kratky–Porod (KP) wormlike chain¹⁴ and being given by

$$f_{S,KP}(L) = \frac{L}{6} - \frac{1}{4} + \frac{1}{4L} - \frac{1}{8L^2} (1 - e^{-2L}) \quad (8)$$

According to the QTP scheme or the Yamakawa–Stockmayer–Shimada (YSS) theory,^{6,15–17} $\langle S^2 \rangle$ for the (perturbed) HW chain of total contour length L with excluded volume is given by

$$\langle S^2 \rangle = \langle S^2 \rangle_0 \alpha_S^2 \quad (9)$$

where the gyration-radius expansion factor α_S may be

given by the Domb–Barrett equation¹⁸

$$\alpha_S^2 = [1 + 10\tilde{z} + (70\pi/9 + 10/3)\tilde{z}^2 + 8\pi^{3/2}\tilde{z}^3]^{2/15} \times [0.933 + 0.067 \exp(-0.85\tilde{z} - 1.39\tilde{z}^2)] \quad (10)$$

with the scaled excluded-volume parameter \tilde{z} defined by

$$\tilde{z} = (3/4)K(\lambda L)z \quad (11)$$

in place of the conventional excluded-volume parameter z . The latter is defined by

$$z = (3/2\pi)^{3/2} (\lambda B)(\lambda L)^{1/2} \quad (12)$$

where

$$B = \beta/a^2 c_\infty^{3/2} \quad (13)$$

with β being the binary cluster integral between beads with a their spacing (in the touched-bead model) and

$$c_\infty = \lim_{\lambda L \rightarrow \infty} (6\lambda \langle S^2 \rangle_0 / L) = \frac{4 + (\lambda^{-1} \tau_0)^2}{4 + (\lambda^{-1} \kappa_0)^2 + (\lambda^{-1} \tau_0)^2} \quad (14)$$

In eq 11, the coefficient $K(L)$ is given by

$$K(L) = \frac{4}{3} - 2.711L^{-1/2} + \frac{7}{6}L^{-1} \quad \text{for } L > 6$$

$$= L^{-1/2} \exp(-6.611L^{-1} + 0.9198 + 0.03516L) \quad \text{for } L \leq 6 \quad (15)$$

Note that L is related to the degree of polymerization x by the equation

$$L = xM_0/M_L \quad (16)$$

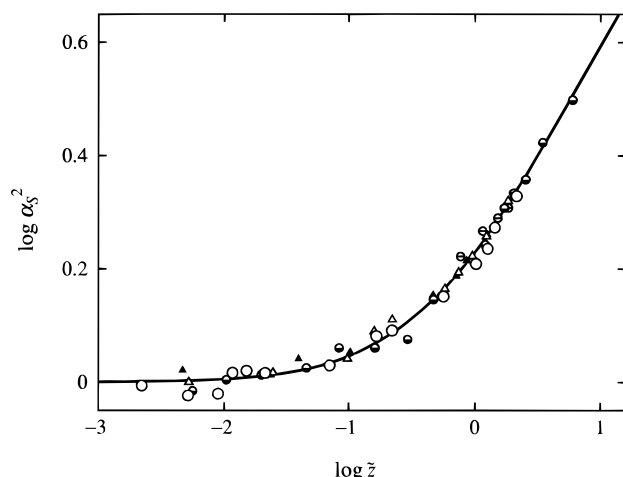
where M_0 is the molecular weight of the repeat unit.

In the previous paper,⁹ we analyzed the experimental values of $\langle S^2 \rangle_{\Theta}/x_w$ for the four PIB samples PIB40 through PIB180 in IAIV at 25.0°C (Θ) (filled circles in Figure 1) and obtained $\lambda^{-1} = 14.0 \text{ \AA}$, assuming that the PIB chain may be represented by the KP chain ($\kappa_0 = 0$) and that the value of M_L is equal to 24.1 \AA^{-1} corresponding to its 8_3 helix taken in the crystalline state. The value of the parameter λB was also determined there to be 0.083 from an analysis of the experimental values of α_S by the use of the YSS theory. In this paper, we analyze simultaneously those unperturbed values (with $\langle S^2 \rangle_{\Theta} = \langle S^2 \rangle_0$) and the perturbed values (unfilled circles in Figure 1) by the use of the above HW theories without and with the excluded-volume effect, respectively, and then determine the five parameters $\lambda^{-1}\kappa_0$, $\lambda^{-1}\tau_0$, λ^{-1} , M_L , and λB by the curve fitting. In Figure 1, the lower and upper solid curves represent the best-fit HW theory values so obtained for the unperturbed and perturbed (YSS) chains, respectively. The former values have been calculated from eq 3 with eqs 4–8 and 16 with the values of the HW model parameters, $\lambda^{-1}\kappa_0 = 1.0$, $\lambda^{-1}\tau_0 = 0$, $\lambda^{-1} = 15.3 \text{ \AA}$, and $M_L = 20.9 \text{ \AA}^{-1}$, and the latter values from eq 9 with eqs 3–8 and 10–16 with the above parameter values and $\lambda B = 0.090$. The value of λ^{-1} is somewhat larger than the previous one, and that of M_L is rather close to 21.6 \AA^{-1} , corresponding to its chain fully extended to the all-trans conformation. The determination of $\lambda^{-1}\kappa_0$ and $\lambda^{-1}\tau_0$ is rather ambigu-

Table 3. Values of α_S , α_η , and α_H for Oligo- and Polyisobutylenes in *n*-Heptane at 25.0 °C

sample	x_w	α_S	α_η^b	α_H^c
OIB11	11.4	0.99		
OIB14	14.1		1.00	
OIB14a	15.3	0.98		
OIB18	18.0		1.01	1.01
OIB18a	19.3	0.97		
OIB22	22.2		1.00	
OIB22a	22.1	1.02		
OIB26	26.2		1.00	
OIB26a	27.9		1.01	1.00
OIB26b	25.7	1.03		
OIB32	32.2	1.02	1.01	
PIB1	155		1.03	
PIB1a	101	1.04		
PIB2	295		1.07	
PIB2a	323	1.10	1.07	1.07
PIB3	496	1.12	1.09	
PIB5	866		1.11	1.10
PIB9	1520		1.14	
PIB13	2310		1.16	
PIB13a	2480	1.20	1.16	1.17
PIB40	7540	1.27 ^a	1.24	1.25
PIB60	11300	1.31	1.27	1.25
PIB80	14600	1.37	1.30	1.29
PIB180	31400	1.46	1.37	1.36

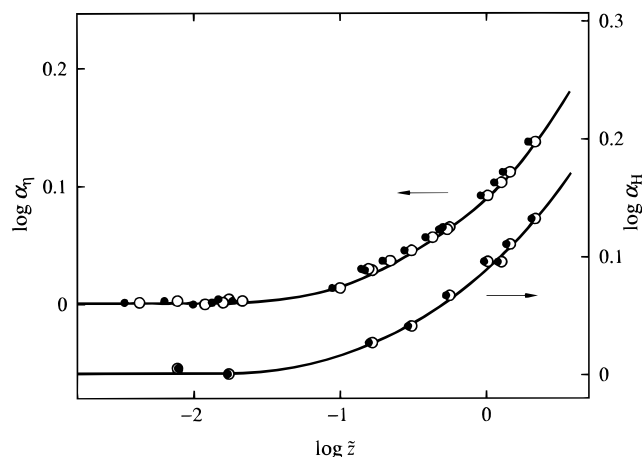
^a The values of α_S for PIB40 through PIB180 have been reproduced from ref 9. ^b The values of α_η have been reproduced from refs 2 and 9. ^c The values of α_H have been reproduced from ref 2.

**Figure 2.** Double-logarithmic plots of α_S^2 against \tilde{z} : (○) PIB in *n*-heptane at 25.0 °C; (◐) a-PS in toluene at 15.0 °C; (△) a-PMMA in acetone at 25.0 °C; (▲) i-PMMA in acetone at 25.0 °C; (◌) PDMS in toluene at 25.0 °C. The solid curve represents the QTP (or YSS) theory values (see the text).

ous, but it is important to note that the KP theory cannot explain the rather steep increase in the observed $\langle S^2 \rangle/x_w$ with increasing x_w in the range of $x_w \lesssim 20$, this leading to the necessity of introducing the weak helical nature⁶ (small finite $\lambda^{-1}\kappa_0$) into the PIB chain.

In the third column of Table 3 are given the values of α_S calculated from eq 9 with the experimental values of $\langle S^2 \rangle$ given in Table 2 and with the corresponding HW theory values of $\langle S^2 \rangle_0$ calculated from eq 3 with eqs 4–8 and 16 with the above parameter values. The values of α_S for the samples PIB40 through PIB180 have been reproduced from Table VI of ref 9, which were calculated from eq 9 with the experimental values of $\langle S^2 \rangle$ and $\langle S^2 \rangle_0 (= \langle S^2 \rangle_0)$ shown in Figure 1.

Figure 2 shows double-logarithmic plots of α_S^2 against \tilde{z} . The unfilled circles represent the above values for PIB in *n*-heptane at 25.0 °C. It also includes the values

**Figure 3.** Double-logarithmic plots of α_η and α_H against \tilde{z} for PIB in *n*-heptane at 25.0 °C: (○) with the values of \tilde{z} calculated with the present values of the HW model parameters; (◐) with the values of \tilde{z} calculated with the previous values of the model parameters (see the text). The solid curves connect smoothly the respective unfilled circles.

previously determined for a-PS in toluene at 15.0 °C (bottom-half-filled circles),¹ a-PMMA in acetone at 25.0 °C (unfilled triangles),⁷ i-PMMA in acetone at 25.0 °C (filled triangles),⁸ and poly(dimethylsiloxane) (PDMS) in toluene at 25.0 °C (unfilled circles with horizontal bars).¹⁹ The solid curve represents the QTP (or YSS) theory values calculated from eq 10. There is seen to be good agreement between theory and experiment, as is natural from the procedure of evaluating \tilde{z} .

α_η and α_H as Functions of \tilde{z} . In the fourth and fifth columns of Table 3 are also given the values of α_η and α_H , respectively, for PIB in *n*-heptane at 25.0 °C, which have been reproduced from Table 6 of ref 2 and Table VI of ref 9 and from Table 6 of ref 2, respectively. In the previous studies of α_η and α_H of PIB in *n*-heptane at 25.0 °C,^{2,7,9} the values of \tilde{z} were calculated from eq 11 with eqs 12 and 16 with the KP (and 8_3 helix) values of the model parameters, $\lambda^{-1}\kappa_0 = 0$, $\lambda^{-1} = 14.0$ or 12.7 Å, and $M_L = 24.1$ Å⁻¹, and with $\lambda B = 0.083$, where the latter value 12.7 Å of λ^{-1} was determined from an analysis of $[\eta]_\Theta$ ¹¹ instead of $\langle S^2 \rangle_\Theta$. The values of α_η and α_H for PIB in *n*-heptane at 25.0 °C are double-logarithmically plotted against \tilde{z} in Figure 3, where the results with the previous and present values of \tilde{z} are shown by the filled and unfilled circles, respectively. We note that the previous \tilde{z} values have been calculated with $\lambda^{-1} = 14.0$ Å for α_η and with $\lambda^{-1} = 12.7$ Å for α_H and that the present \tilde{z} values have been calculated with the present values of the HW model parameters, i.e., $\lambda^{-1}\kappa_0 = 1.0$, $\lambda^{-1}\tau_0 = 0$, $\lambda^{-1} = 15.3$ Å, $M_L = 20.9$ Å⁻¹, and $\lambda B = 0.090$. In the figure, the solid curves connect smoothly the respective unfilled circles. It is seen that the re-evaluation of \tilde{z} shifts the data points to the right in the range of $\tilde{z} \gtrsim 0.1$.

Figure 4 shows double-logarithmic plots of α_η and α_H against \tilde{z} for PIB with the present values of the model parameters and also for a-PS in toluene at 15.0 °C,^{1,3,4} a-PMMA in acetone at 25.0 °C,^{5,7} and i-PMMA in acetone at 25.0 °C.^{5,8} The symbols have the same meaning as those in Figure 2. The solid curves represent the theoretical values of α_η in the QTP scheme calculated from the Barrett expression²⁰

$$\alpha_\eta^3 = (1 + 3.8\tilde{z} + 1.9\tilde{z}^2)^{0.3} \quad (17)$$

with \tilde{z} in place of z . It is seen that the data points form

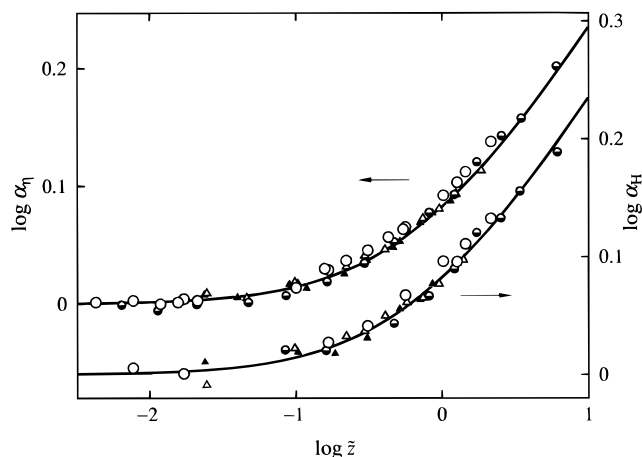


Figure 4. Double-logarithmic plots of α_η and α_H against \tilde{z} . The symbols have the same meaning as those in Figure 2. The solid curves represent the theoretical values of α_η calculated from eq 17.

a single-composite curve within experimental error in each case and that they may be well reproduced by the above theoretical values in both cases. Clearly, the results are better than before (compare with Figure 7 of ref 2, Figure 8 of ref 7, and Figure 6 of ref 9). Thus the consistency of the results for PIB with those for the other polymers has been improved.

Concluding Remarks

We have determined the HW model parameters for the PIB chain by analyzing the present data for $\langle S^2 \rangle$ obtained from SAXS and LS measurements in *n*-heptane at 25.0 °C together with the previous data⁹ obtained from LS measurements for large M_w in the same solvent condition and also in IAIV at 25.0 °C (Θ), by the use of the HW theories with and without the excluded-volume effect.⁶ With these parameter values for PIB, the plots of α_η and α_H against the scaled excluded-volume parameter \tilde{z} for PIB along with those for a-PS and a- and i-PMMA are shown to form a single-composite curve better than before in each case, confirming the validity of the QTP scheme that all the expansion factors are functions only of \tilde{z} irrespective of the polymer-solvent system. The consistency of the results for PIB with those for the other polymers has been improved by the re-evaluation of \tilde{z} .

Finally, we must make a remark on the case of PDMS,¹⁹ for which the data points for α_H plotted against \tilde{z} also deviate somewhat upward from the above single-composite curve. The situation is more complicated for this polymer than for PIB, since the hydrodynamic bead diameters are different in the good and Θ solvents used, and since then α_η and α_H cannot be determined directly from the observed $[\eta]$ and D . Thus the difficulty in the case of PDMS does not arise from the values of the HW model parameters (or of \tilde{z}) but rather from the *experimental* values of α_η and α_H themselves estimated by means of the HW transport theories.^{6,19}

References and Notes

- (1) Abe, F.; Einaga, Y.; Yoshizaki, T.; Yamakawa, H. *Macromolecules* **1993**, *26*, 1884 and succeeding papers.
- (2) Osa, M.; Abe, F.; Yoshizaki, T.; Einaga, Y.; Yamakawa, H. *Macromolecules* **1996**, *29*, 2302.
- (3) Arai, T.; Abe, F.; Yoshizaki, T.; Einaga, Y.; Yamakawa, H. *Macromolecules* **1995**, *28*, 3609.
- (4) Arai, T.; Abe, F.; Yoshizaki, T.; Einaga, Y.; Yamakawa, H. *Macromolecules* **1995**, *28*, 5458.
- (5) Arai, T.; Sawatari, N.; Yoshizaki, T.; Einaga, Y.; Yamakawa, H. *Macromolecules* **1996**, *29*, 2309.
- (6) Yamakawa, H. *Helical Wormlike Chains in Polymer Solutions*; Springer: Berlin, 1997.
- (7) Abe, F.; Horita, K.; Einaga, Y.; Yamakawa, H. *Macromolecules* **1994**, *27*, 725.
- (8) Kamijo, M.; Abe, F.; Einaga, Y.; Yamakawa, H. *Macromolecules* **1995**, *28*, 1095.
- (9) Abe, F.; Einaga, Y.; Yamakawa, H. *Macromolecules* **1993**, *26*, 1891.
- (10) Horita, K.; Abe, F.; Einaga, Y.; Yamakawa, H. *Macromolecules* **1993**, *26*, 5067.
- (11) Abe, F.; Einaga, Y.; Yamakawa, H. *Macromolecules* **1991**, *24*, 4423.
- (12) Konishi, T.; Yoshizaki, T.; Saito, T.; Einaga, Y.; Yamakawa, H. *Macromolecules* **1990**, *23*, 290.
- (13) Yamakawa, H.; Fujii, M. *J. Chem. Phys.* **1976**, *64*, 5222.
- (14) Kratky, O.; Porod, G. *Recl. Trav. Chim. Pays-Bas* **1949**, *68*, 1106.
- (15) Yamakawa, H.; Stockmayer, W. H. *J. Chem. Phys.* **1972**, *57*, 2843.
- (16) Yamakawa, H.; Shimada, J. *J. Chem. Phys.* **1985**, *83*, 2607.
- (17) Shimada, J.; Yamakawa, H. *J. Chem. Phys.* **1986**, *85*, 591.
- (18) Domb, C.; Barrett, A. J. *Polymer* **1976**, *17*, 179.
- (19) Horita, K.; Sawatari, N.; Yoshizaki, T.; Einaga, Y.; Yamakawa, H. *Macromolecules* **1995**, *28*, 4455.
- (20) Barrett, A. J. *Macromolecules* **1984**, *17*, 1566.

MA970738+